International Conference on Space Optics—ICSO 2020

Virtual Conference

30 March–2 April 2021

Edited by Bruno Cugny, Zoran Sodnik, and Nikos Karafolas

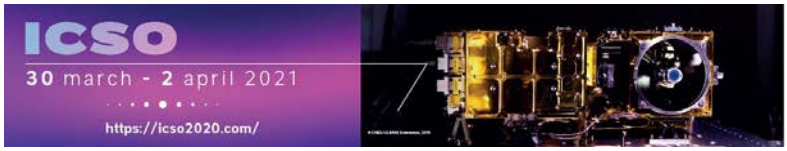

The challenges of broadband performances within a compact imaging spectrometer: the ELOIS solution

International Conference on Space Optics — ICSO 2020, edited by Bruno Cugny, Zoran Sodnik, Nikos Karafolas, Proc. of SPIE Vol. 11852, 118521E · © 2021 ESA and CNES
CCC code: 0277-786X/21/$21 · doi: 10.1117/12.2599239

The challenges of broadband performances within a compact imaging spectrometer: the ELOIS VISWIR solution

Benoit Borguet*[a], Vincent Moreau[a], Stefano Santandrea[b], Jorg Versluys[b], Arnaud Bourdoux[c]
[a]AMOS, 2 Rue des Chasseurs Ardennais, 4031 Angleur, Belgium; [b]ESTEC, The Netherlands;
[c]Spacebel, 6 Rue des Chasseurs Ardennais, 4031 Angleur, Belgium

ABSTRACT

ELOIS VISWIR is a science-grade, smallsat compatible, pushbroom hyperspectral payload covering the entire VISWIR spectral range (400-2450 nm) with over 200 contiguous 10 nm wide spectral bands. Its unique all reflective optical design enables covering a 70 km swath with 35 m ground sampling distance (GSD), while guaranteeing high imaging performances across the full field of view.

At the core of the instrument, the spectrometer formula expands upon AMOS' state of the art Offner-based ELOIS VNIR long-slit spectrometer [1], including key features such as built-in slit de-magnification, and the use of a fine-tuned freeform diffraction grating enabling the appropriate compensation of the optical aberrations affecting the fast, F/2.1 focal plane.

Besides its excellent imaging performances and advanced control of distortions, the ELOIS VISWIR delivers unparalleled throughput in a single optical chain thanks to the inclusion of leading-edge technical solutions including a broadband multi-blazed freeform diffraction grating, a variable dichroic beam-splitter plate, and high efficiency order sorting filters. In this paper, we discuss these key ingredients in the optical design of the ELOIS VISWIR spectrometer and report the optical performances of the manufactured optical components.

Keywords: Hyperspectral imager, spectrometer, freeform optics, diffraction grating, VISWIR

1. INTRODUCTION

The development of high quality hyperspectral remote sensing instrumentation has stirred a significant interest among the scientific community over the last decades owing to its unique ability in deriving detailed quantitative surface characteristics (see e.g. [2] and references therein). Applications enabled by the continuous spectral monitoring of the Earth's environment include a broad range of scientific investigations such as tracing biophysical and biochemical parameters from the terrestrial vegetation, urban analysis including pollution monitoring or land management, and precision agriculture to atmospheric chemistry.

A slew of space-based hyperspectral missions has emerged over the years (among others HySUI, EnMap, PRISMA, AHSI, HyspIRI, or CHIME) aiming at the accurate spectroscopic measurements over the VISWIR spectral range (400-2500 nm) see [2][9]. Common to these missions are the high SNR performances (typically > 400 in the VNIR and > 200 in the SWIR for a 0.3 albedo reference scene) over the 200+ contiguous 10 nm spectral bands. The spatial resolution is of the order of 30 m and the covered swath is of the order of 30 km (excepting for CHIME and HyspIRI). The optical design of the spectrometers relies mainly on the Dyson formula (HyspIRI), Offner based layout (HySUI, CHIME), or complex hybrid optical schemes (EnMap, PRISMA).

ELOIS VISWIR [6] is the compact hyperspectral imager payload developed by AMOS, providing a small-sat compatible alternative to the major hyperspectral instruments. It covers the 400-2450 nm spectral range with a spectral resolution of 10 nm (2.5 in un-binned mode in the VNIR) exhibiting SNR performances rivalling with bigger missions such as EnMap or PRISMA. Further it resolves ground-projected pixels of 35m (GSD) at Nadir in the VNIR and 70m to 35m in the SWIR (depending on sensor availability) over a swath of 70 km. The main specifications of the payload are given in Table 1. In the Section 2 we detail the optical design of the spectrometer focusing on technologies enabling high

throughput along with good image quality. In Section 3 we report the nominal performances of the spectrometer. In Section 4 we report the performances of the as-built critical spectrometer components.

Table 1 : ELOIS VISWIR Payload Specifications

Specification	Requirement
Reference orbit	642 km
Ground Sampling Distance	35 m
Swath	70 km
SNR (alb. 0.3)	>400(VNIR); > 150 (SWIR)
Spectral Range	400-2450 nm
Spectral bands	Up to 210
Spectral resolution	2.5 nm – 10 nm

2. OPTICAL DESIGN

The complete ELOIS VISWIR instrument is composed of three major subsystems: the front telescope, the spectrometer unit, and the spectrometer focal planes. The availability of specific VNIR and SWIR sensors with adequate performances in terms of pixel size, pixel count, frame rate, and full well, limits the high level architecture of the instrument. This point as well as the overall design of the complete instrument has been detailed in [6], so only the spectrometer design will be discussed here.

The key driver in the elaboration of the ELOIS VISWIR long-slit spectrometer optical design has been the maximization of the optical throughput over the complete 400-2450 nm spectral range while preserving the necessary compactness ensuring its compatibility with a small-sat based mission. Therefore the optical formula builds upon customized Offner-Chrisp configuration: a three mirror anastigmat configuration in which the secondary mirror is replaced by a convex freeform diffraction grating enabling the resolved spectral imaging of the slit onto the focal plane. A major departure from the proposed design with traditional Offner-based spectrometers is the inclusion of a built-in slit de-magnification function of M=-0.6. This de-magnification benefits the overall SNR in the sense that it allows using a larger slit for a fixed pixel size, virtually increasing the number of photons impinging each pixel by a factor $1/M^2$. The spectrometer input slit is 52.2 mm long by 25.8 µm wide matching the dedicated 2022 x 256 15.5 µm square pitch VNIR sensor described in Moreau et al. 2018. Note that as a corollary, the de-magnification also relaxes the constraints on the fore optical train elements through the increase of its F# by a factor 1/M.

The extension of the original ELOIS design to the VISWIR spectral range considers the “Combined VNIR/SWIR spectrometer” configuration proposed in [7][8]: both VNIR and SWIR channels are integrated in a single spectrometer where a beam splitter placed after the imaging mirror creates the necessary spatial separation of the reflected VNIR and transmitted SWIR band to their dedicated focal planes. In this configuration, a unique convex grating diffracts the SWIR in the first order (m=-1) and the VNIR in the second (m=-2). The spectral dispersion in the VNIR is thus twice the dispersion in the SWIR. For ELOIS VISWIR the 37.66 groove/mm grating enables a spectral sampling of 2.5 nm/pixel in the VNIR, while a spectral sampling of 5 nm/pixel could be achieved in the SWIR pending the existence of compliant 15µm pitch pixel sensor.

The raytrace of the VISWIR spectrometer is presented in Figure 1: the spectrometer optical design comprises the input slit, two highly aspherical mirrors, a freeform diffraction grating, a beam splitter assembly and separate VNIR and SWIR focal planes. An additional folding mirror has been added improving the system compactness. The essential technologies enabling the radiometric performances of this broadband, compact spectrometer are discussed in the following sections.

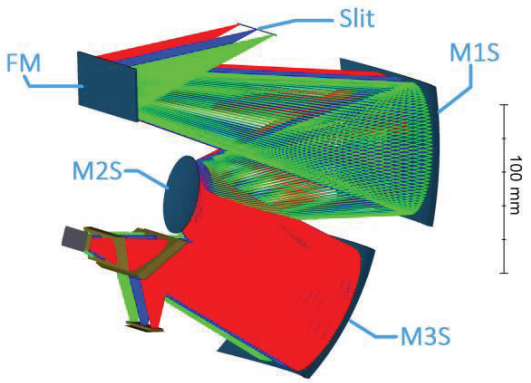

Figure 1: Raytrace of the ELOIS VISWIR spectrometer. The optical design comprises an input slit, a folding mirror, collimating and imaging highly aspherical mirrors (M1S and M3S), a convex freeform diffraction grating (M2S), a beam splitter assembly (brown plates), and the VNIR and SWIR focal planes.

2.1 Broadband Freeform Diffraction Grating

At the heart of the VISWIR spectrometer lies a 36.77 grooves/mm convex freeform diffraction grating. It fulfills several roles in addition of providing the traditional spectral dispersion of the input slit image. First, while conventional 1:1 Offner based spectrometer offer by their singular symmetry an excellent level of control of aberrations and distortions, the asymmetry brought in the optical design by the de-magnifying function necessitates the introduction extra degree of freedom in order to preserve the imaging quality of the instrument. Proposed solution consist in the introduction of fine-tuned aberrations over the grating aperture (the pupil of the system) enabling the balancing of the resulting aberrations over the large focal plane. Even more so when considering the fast speed at the focal plane (F#2.1), wide spectral range, and associated 52.2 mm long input slit. As shown in [1], reaching adequate imaging performances does not require strong freeformity of the grating substrate. Indeed, the deviation to the best fitting sphere encountered over the 40 mm diameter useful area of the ELOIS VISWIR grating is merely <10 µm PtV while the slope deviation remains below ~1 mrad. Therefore, while being freeform, the grating SFE can be tested using a regular null test with a matching reference sphere, without requiring the use of any CGH, see Figure 2.

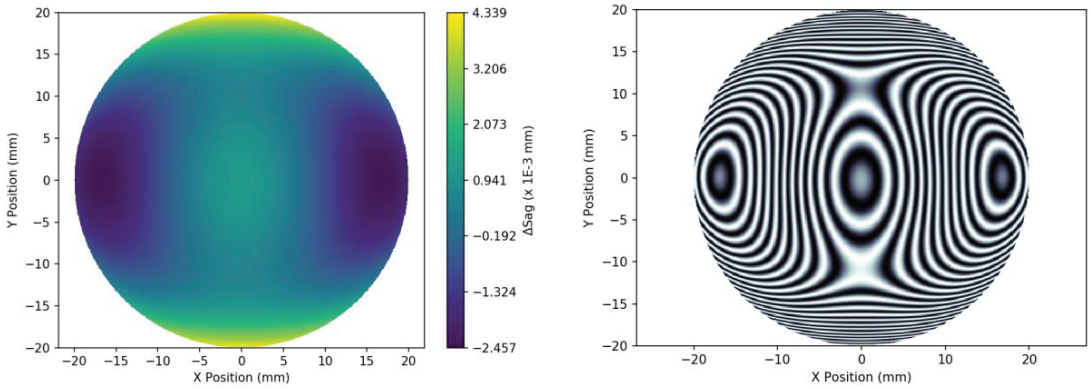

Figure 2: Left: the freeform departure from the best fit sphere of the ELOIS VISWIR grating is rather limited and remains below 10 µm PtV over the useful grating aperture. Right: The smooth freeform profile enables testing the surface form accuracy against a regular spherical reference wavefront without producing unresolved fringes.

Secondly, feeding both VNIR and SWIR channels, the diffraction grating must exhibit substantial spectral response over the complete 400-2450 nm spectral range. A first strategy enabling an increase of the grating efficiency is performed through a "photon recycling scheme", where photons diffracted in order m=-1 are transmitted towards the SWIR sensor, while photons diffracted in order m=-2 are reflected towards the VNIR sensor. However the broadband response cannot

be matched by a single blazed grating, more specifically in the VNIR spectral range in which the bandwidth of the single blaze grating in diffracted order m=-2 does not allow achieving sufficient throughput at the shortest and longest wavelengths of the spectral range simultaneously. Further, a single blaze configuration does not allow pushing the throughput around 400 nm while preserving significant response above 2000 nm in diffracted order m=-1.

The grating being located at the pupil, a solution for broadening its spectral efficiency consists in the split of the useful grating area into distinct blaze regions. The extra freedom provided by the multiple blaze wavelengths and relative area enables the fine-tuning of the grating efficiency in both diffracted orders over the spectral range, matching the target SNR. For ELOIS VISWIR the grating surface is divided into two blaze regions (Zone A and B) with blaze wavelengths of 900, and 1420 nm occupying respectively 45% and 55% of the useful area. Both blaze area are phase-matched during ruling, so that the mean phase difference over the full pupil is minimized. Note that since the grating is the pupil of the spectrometer, the variation of the efficiency encountered over both blaze regions at specific wavelengths is considered as pupil apodization. However, Zemax simulations show that the limited number of blaze regions, and relative sizes do not produce appreciable effect on the instrument point spread function.

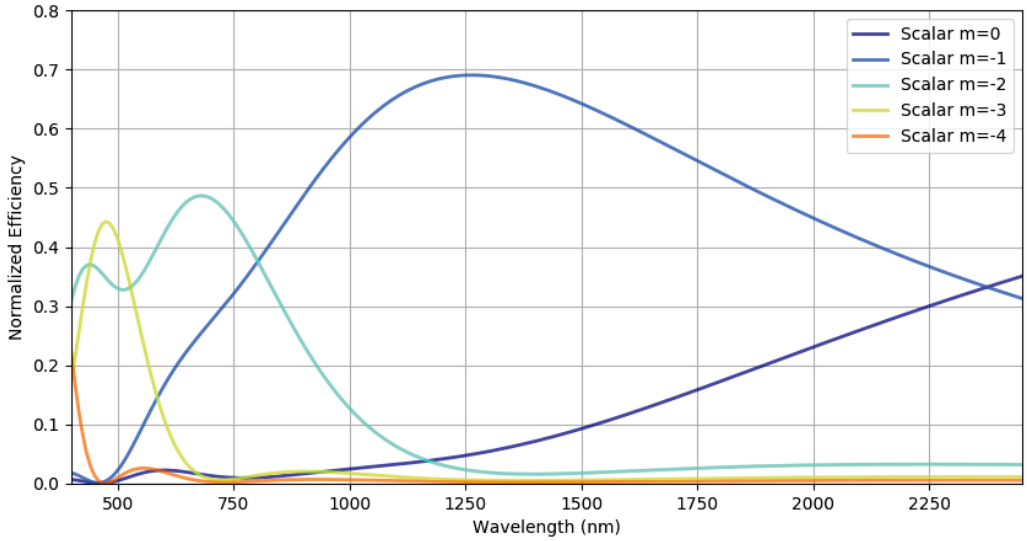

Figure 3: Diffraction efficiency (scalar theory) for the multi-region blazed ELOIS VISWIR grating. The use of two distinct blaze regions enables reaching a satisfying throughput over both VNIR and SWIR spectral ranges in diffracted orders m=-2, and m=-1 respectively. We further note significant throughput around 500 nm and 400 nm for the spurious diffracted orders m=-3 and m=-4.

2.2 Variable Dichroic Beam-Splitter

The beam splitter is an essential component of the VISWIR spectrometer design, operating the spatial separation of the VISWIR spectral range into separate VNIR and SWIR focal planes. The beam splitter assembly is composed of a wedged dichroic beam splitter plate (BSP) and a wedged compensator plate (CP) placed at an angle, both made in INFRASIL. The CP compensates for the astigmatism building up during the transmission of the fast converging F#2.1 SWIR beam through the BSP.

The frontface of the BSP is coated with a specific dichroic coating ensuring a high reflectivity of the VNIR beam altogether with a high transmission of the SWIR. The coating stack is composed of more than a hundred layers of alternatively high refractive index TiO_2 and low refractive index SiO_2. The spectral efficiency of the transmission and reflection is function of the Angle of Incidence (AOI) of the impinging light ray on the coating. In the ELOIS VISWIR design, the speed in the focal plane area is such that the nominal AOI on the beam splitter plate typically ranges from 20 to 50° for any sub-pupil. Considering experimental transmission and reflection efficiencies (Optics Balzers Jena, see top panel of Figure 4), we compute the biconical value of the spectral response expected for the dichroic BSP to present a ~100 nm gap between the useful VNIR and SWIR beams. Therefore, no accurate radiometric data could be acquired over the 900-1000 nm dichroic transition spectral range.

Reduction of the dead region bandwidth could be achieved by applying a monotonic thickness varying dichroic coating in the spectral direction. The varying-thickness coating allows a local shift the transition wavelength for specific AOI as a function of the spectral position on the BSP. However due to the fact that the sub-pupils for a selected field of view corresponding to different wavelengths are partially spatially co-located on the BSP, we use as best approximation an average linear AOI distribution on the BS surface, corresponding to a monotonically varying coating thickness in the y-direction. This approximation mimics the overall spectral axis AOI distributions for wavelengths/diffraction orders couple within the nominal operating range of the ELOIS VISWIR spectrometer. The use a fine-tuned coating enables restricting the dead region to the 900-960 nm spectral region (see bottom panel of Figure 4), coincident with water vapor absorption line in the reflected sun radiance spectrum observed by the instrument.

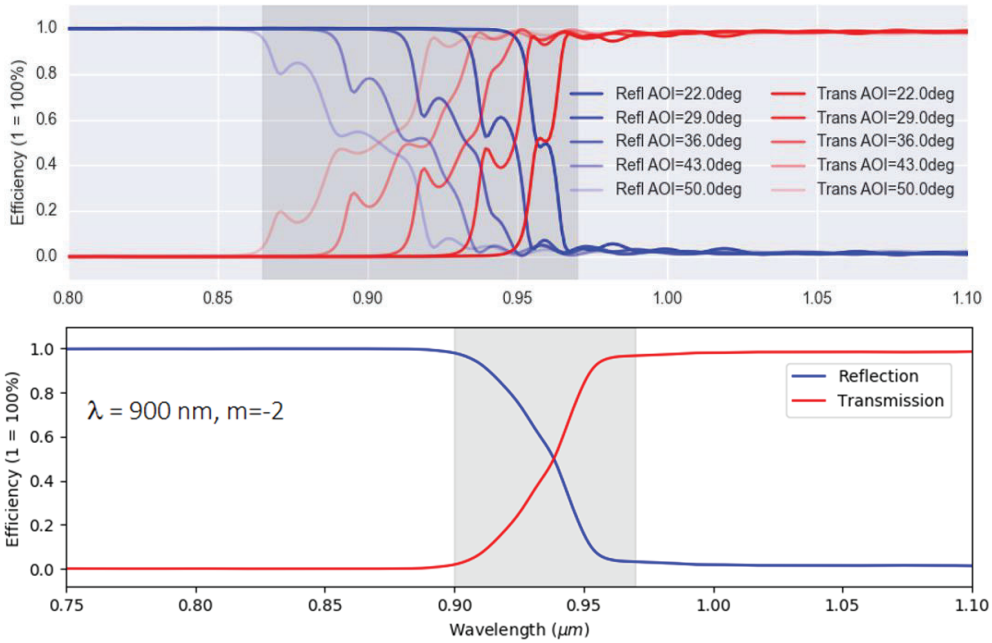

Figure 4: Top: Experimental efficiency curves for a dichroic coating considering various AOI (OBJ). Using constant thickness dichroic coating on the BSP would lead to a dead region of ~100 nm. Bottom: considering a monotonically thickness varying coating along the spectral direction reduces the dead region to about 60 nm for any sub-pupil (900 nm in VNIR order m=-2 is shown here).

2.3 High efficiency Sorting Filters

While channeling VNIR and SWIR photons towards appropriate focal planes, the carefully crafted dichroic beam splitter coating does not free the light impinging both VNIR and SWIR sensors from being corrupted with the spurious diffracted orders, thereby increasing the crosstalk between unrelated bands and compromising the accurate radiometry of the scene. Placing finely tuned order sorting filters in front of both sensors allows spatially rejecting wavelengths that would reach inappropriate sensor bands. Specific VNIR and SWIR filters are developed, and deposited on plane parallel BK7G18, and INFRASIL substrates respectively. Given the dispersion and speed of the spectrometer, the backface of the filters are coated, leading to reduced footprints of the useful beam.

In the VNIR channel, the rejection filter (OSV) should ensure the rejection of light diffracted in all orders excepting order m=-2. However in that spectral region, the multi-region blaze grating exhibits high diffraction efficiencies in spurious orders m=-3 and -4 for wavelengths below 500 nm, and of order m=-1 for wavelengths above 500 nm, requiring an overall optical density > 3 (goal >4) to ensure satisfying rejection properties. In Figure 5 we devise the spectro-spatial function of the rejection coating applied to the OSV. We consider the interference of spurious diffracted orders m = 0, -1, -3, -4 and -5 relative to the nominal VNIR arm m = -2 order. Appropriate rejection could be reached using a set of four hi and lo-pass filters. In the SWIR, the nominal diffracted order is m=-1. Only a single hi pass filter could provide the needed rejection of the spurious m < -1 diffracted light.

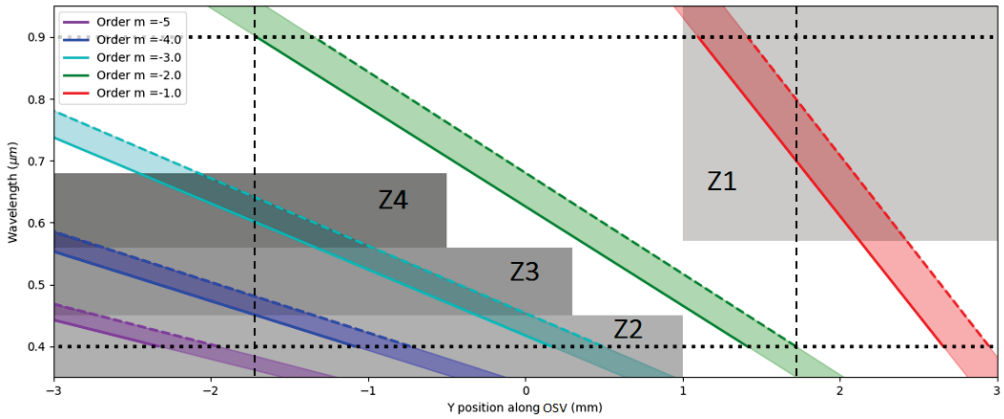

Figure 5: Defining the spectro-spatial rejection law on the OSV. The shaded green area represents the footprint of the useful beam at selected positions on the OSV (dispersion axis). Spurious orders footprints are represented in different colors. A set of four hi and lo-pass regions could enable reaching the desired rejection function.

3. SPECTROMETER PERFORMANCES

SNR and image quality performances governed the design architecture and optimization so that the ELOIS VISWIR design offers exquisite throughput and optical performances in a compact volume through the use of a freeform grating based design (see [6]). Specifically, the radiometric performance stems from both the achieved small F-number and the complex broadband diffraction grating configuration relying on multi-order and multi-region blaze configuration, simultaneously maximizing the grating efficiency over VNIR and SWIR spectral ranges. the filters are coated, leading to reduced footprints of the useful beam.

A comprehensive radiometric model of the ELOIS VISWIR has been composed predicting the SNR performances of the system considering a 10 nm bandwidth for each spectral channel. It includes the at-sensor upwelling radiance, the transmission properties of all optical elements, the diffraction efficiency model for the multi-region grating as well as the properties of the sensors. Note that at the operating frame rate suited for a 35 m GSD instrument flying on a LEO platform, the shot noise remains the largest contributor when dealing with large number of photon statistics and high performance sensors. In Figure 6, we illustrate the expected SNR in the VNIR and SWIR spectral ranges considering three potential radiance scenario, the reference being a nadir looking configuration with an albedo of 0.3 and a sun zenith angle of 30°. In the VNIR, a SNR~400 is reached in the 450-750 nm spectral range, and then linearly decreasing to ~150 at 900 nm. In the SWIR, the dual-order photon recycling scheme provides a wealth of photons at the shortest wavelengths. A SNR > 180 is typically reached over the 970-2200 nm spectral range.

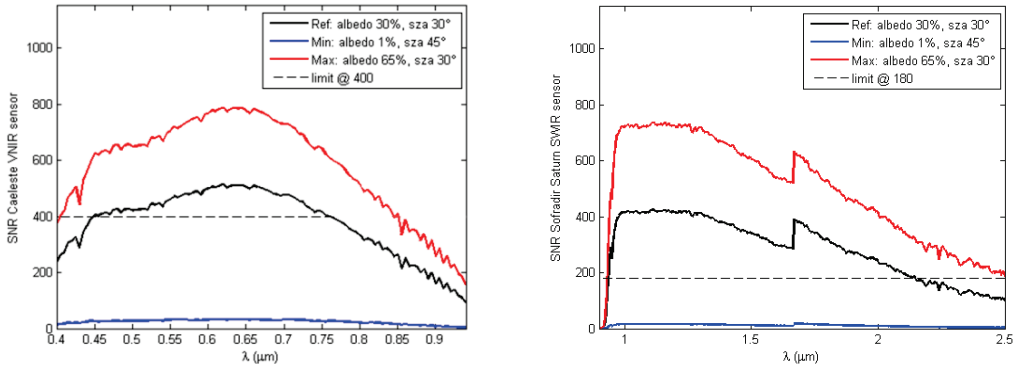

Figure 6: Predicted SNR performances for the ELOIS VISWIR for three nadir looking scenarios at the VNIR (left) and SWIR right) focal planes. The reference scenario considers an albedo of 0.3 and a 30° sun zenith angle. The black dashed line indicates the mission specification in the reference case. The jump in the SWIR SNR occurring around 1700 nm is associated with a change in the gain of the sensor operated to prevent sensor saturation for shorter wavelengths.

4. AS BUILT OPTICAL ELEMENTS

The state of the art optical and radiometric performances of the ELOIS VISWIR rely on three key technologies enabling the optical design detailed in Section 2. In this section we report the optical performances of the manufactured grating, varying beam splitter coating, and VNIR order sorting filter. The diffraction grating has been manufactured by AMOS, while the optical coatings have been designed and applied by Optic Balzers Jena.

4.1 Broadband Diffraction Grating Performances

The multi-region convex freeform diffraction grating has been manufactured at AMOS using Single Point Diamond Turning. The grating substrate is AlSi on top of which a thin layer of NiP is applied, in which the grooves and the freeform shape are etched. Both blaze regions are co-phased during the machining. In Figure 7 we report the measurement of the grating surface form error against a reference spherical wavefront. The test is conducted at 632.88 nm explaining the variation of contrast observed between both blaze regions. The freeform substrate is in line with the nominal shape over the useful grating area. We report a deviation of the machined profile from the theory of 68 nm RMS, of which 50 nm RMS account for low frequency terms (< Z37) and 40 nm RMS to higher spatial frequencies due to the freeform machining.

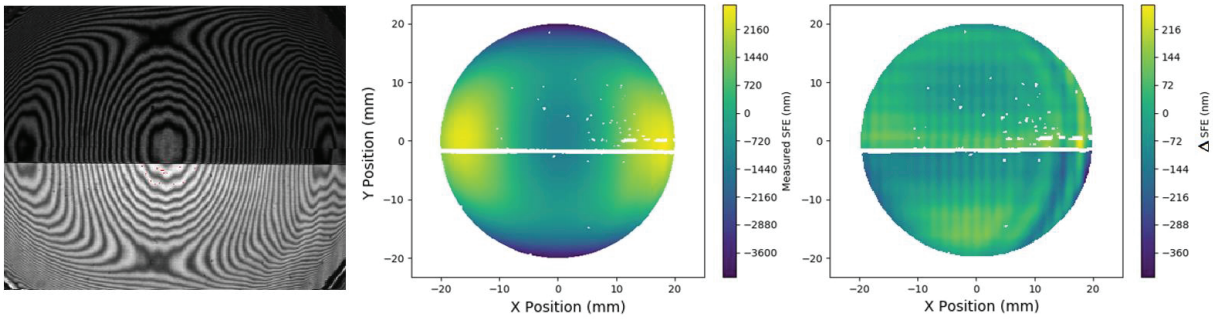

Figure 7: Interferogram of the freeform grating substrate tested against a spherical reference wavefront. The interferometer source is a laser at 632.88 nm so that variation of the fringe visibility over the pupil is caused by the relative efficiency in both blaze-regions. The departure from the freeform design is 68 nm RMS over the useful optical area (rightmost plot).

Confocal microscopy conducted over both regions demonstrate the groove periodicity has been achieved, and that the blaze angles are in good agreement with the specification in both regions. This latter observation is further confirmed by the measurement of the diffraction efficiency in orders m=-1 and m=-2 over the accessible spectral range by our test setup. The setup test consists of a polychromatic light source, a series of narrow band filters (10 to 12 nm bandwidth), an Offner relay and a CMOS and InGaAs focal plane. Switching of the secondary unstructured reference mirror in the relay, by the freeform grating enables computing the relative efficiency of the grating over the 400-1400 nm spectral range. The results are presented in Figure 8.

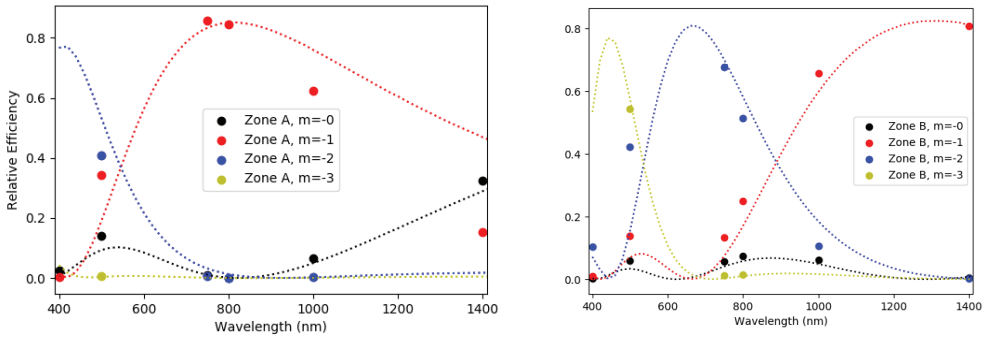

Figure 8: Measured grating efficiencies over blaze region Zone A (left) and B (right). Measurements in diffracted orders m=0, -1, -2 and -3 are compared with theoretical predictions of the PC Grate software (dotted lines). The test setup limits the spectral range to 400-1400 nm.

we observe a fair agreement between the measured efficiencies and theoretical predictions from the PC Grate software suggesting a correct blaze angle in both Zone A and B regions of the pupil. We however note a slight overall blueshift (~50 nm) of the measured efficiencies.

4.2 Dichroic Beam Splitter Coating Performances

The dichroic coating of the beam-splitter is designed to provide a high reflectance in the VNIR range (400-900 nm) and a high transmittance in the SWIR range (975 – 2450 nm). In order to minimize the bandwidth of the dead radiometric region between the reflected and transmitted beam, a linearly thickness varying coating has been deposited along the spectral dimension, locally shifting the transition edge, matching the average local AOI.

The challenging confinement of the edge transition in the 900-970 nm spectral region is well achieved, despite the large range of angle-of-incidence associated to the small F/number. The light-grey lines in Figure 9 show the location of the dichroic transition for AOI=48° assuming a constant thickness coating, which lies outside the allowed spectral range. The blue curve is the as-built measured position for that same AOI that has been shifted back in the spectral range observed for the minimal AOI (22°) thanks to this strategy of thickness control. The as-built position of the edge is very close to the design value (black curves) where we report a <10 nm overall shift. The performance of the coating is achieved over the complete VNIR spectral range with reflectivity over 99.5%. In the SWIR the performance is > 90% excepting for the largest AOI at the longest wavelengths (> 2300 nm) where it linearly drops to about 83% at 2500 nm. However the measured transmittance shall be corrected from the impact of Fresnel reflection on the backface since the coating performances have been measured before applying the Anti-reflective coating on that face.

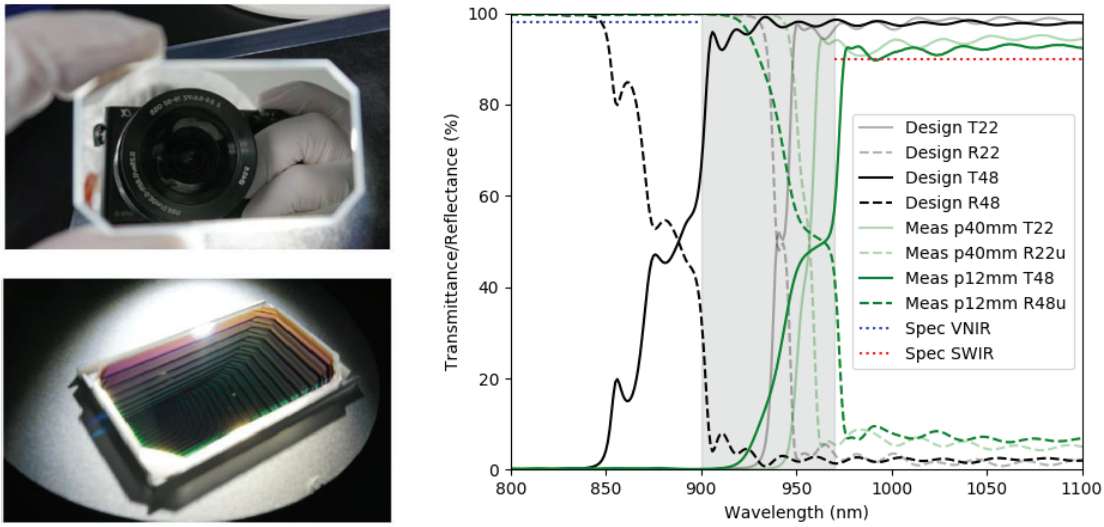

Figure 9: Left: Dichroic beam splitter plate coating as viewed from the front face (Top), and the backface (Bottom, SWIR Anti-reflective coating). Right: Spectral performance of the dichroic coating in the VNIR/SWIR transition region. The thickness varying coating allows a good match between the transition region at extreme AOI over the useful optical area (green lines), the black and grey lines report the transition location for AOI=22° and 48° without thickness variation.

4.3 VNIR Rejection Filter Performance

Currently, only the more challenging VNIR sorting filter has been manufactured. As detailed in Section 2.3, in the VNIR channel, robust rejection of the spurious diffracted orders m=-1, and m < -3 is mandatory. In practice this goal is achieved by using a set of four lo and hi-pass filters arranged in a specific spectro-spatial configuration (see Figure 5) deposited on the backface of the OSV plate, while Anti-reflective coating is applied on the front face. In addition the filter window is partially covered with a black chromium mask, including a set of specific clear windows paired with fiducials etched in the sensor dye and used for co-alignment purpose.

In Figure 10 we compare the design filter transmittance profile with the spectral performances measured on coating samples. The spectral position of the filter transition (half maximum) are respectively 496 nm, 598 nm, 716 nm for the

high pass filters and 629 nm for the low pass filter. We note a slight discrepancy in the transmission of the short pass filter for wavelengths below 450 nm, where the specification is not met. This reduced transmittance is induced by the substrate material, and not the coating itself. Indeed while the addition of Cerium in the G18 space grade BK7 allows a stabilization of the material with respect to radiation, it also attenuates the transmittance of the glass in the blue.

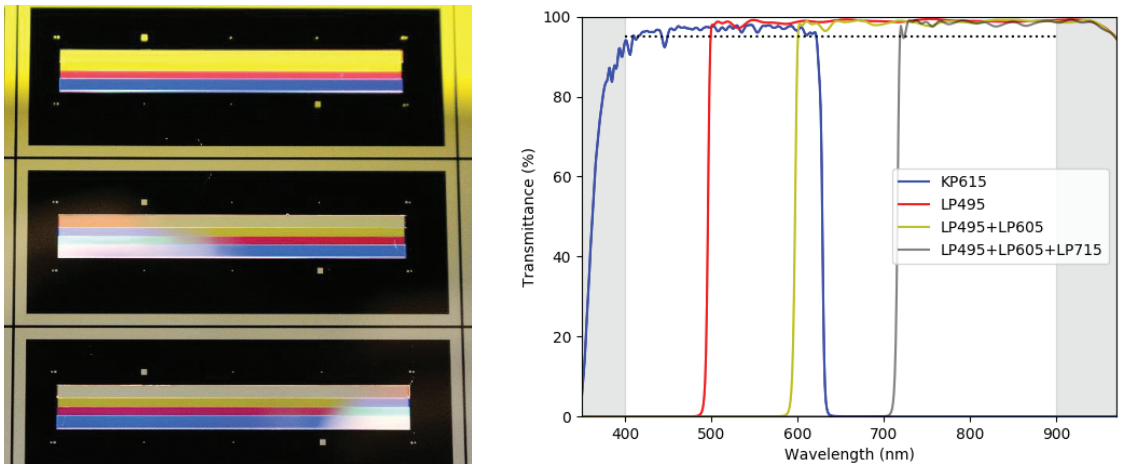

Figure 10: Left: OSV piece-wise filters on their production wafer before cutting. Right: As-built transmittance profile of the hi and lo-pass filters, measured on coating witness samples.

The rejection performances of the coatings are compared in Figure 11. The evidence is provided that the minimum specification of rejection better than OD3 (< 0.1% transmittance) is achieved over the complete VNIR range. The goal value of OD4 (<0.01% transmittance) is even reached over significant portion of the spectral range (specifically between 450-600 nm, and 625-750 nm).

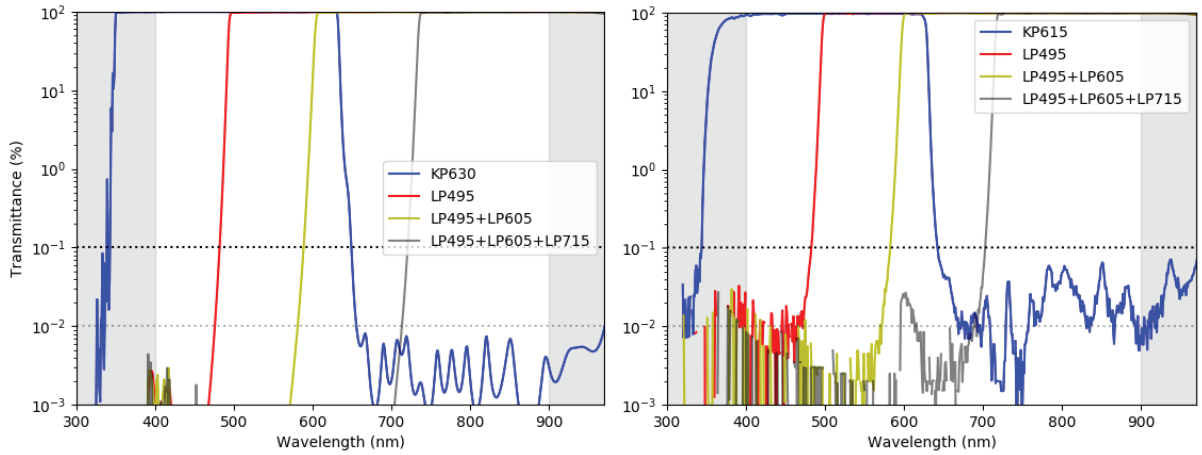

Figure 11: Left: As designed rejection performance for the OSV coatings. The design objective is a rejection below 0.01 %, with a minimal requirement of 0.1% (OD3). Right: As built rejection levels for the OSV measured on witness samples. Rejection below 0.1% is achieved for all filters over the full VNIR spectral range, while OD4 is reached over large portions of the spectrum.

5. CONCLUSIONS

In this paper we discuss the optical design of ELOIS VISWIR: a compact, high performance, smallsat compatible hyperspectral imager. The optical design of the spectrometer is guided by the maximization of the spectral throughput

over the VISWIR spectral range (400-2500 nm).Our analysis focuses on three key technologies enabling state of the art broadband radiometric performances for the spectrometer section of the instrument:

- ⇨ A multi-region blazed freeform diffraction grating
- ⇨ A thickness varying dichroic coating applied to the beam splitter
- ⇨ High performance rejection filters for the VNIR and SWIR channels.

We report the performances for the as-built optical elements, showcasing their manufacturability and associated benefit in the optical design of science-grade Earth observing hyperspectral instrumentation. This new family of compact Spectro-imager can offer valuable solutions for high performances hyperspectral missions on small satellites for earth observation and planetary exploration. The cost-effective approach is also an important advantage in the perspective of the development of future satellites constellations.

REFERENCES

[1] De Clercq, C., Moreau, V., Jamoye, J.F., Zuccaro Marchi, A., and Gloesener, P., « ELOIS : an innovative spectrometer design using a free-form grating", Proc. SPIE 9626, 96261O (2015)
[2] Transon, J., d'Andrimont, R., Maugnard, A., and Defourny, P., « Survey of Hyperspectral Earth Observation Applications from space in the sentinel-2 Context
[3] Marchi, A. Z., and Borguet, B., "Freeform Grating Spectrometers For Hyperspectral Space Applications: Status of ESA Programs," in Optical Design and Fabrication 2017 (Freeform, IODC, OFT), OSA Technical Digest (online), paper JTh2B.5 (2017).
[4] Reimers J., Thompson K.P., Troutman, J., Owen, J. D., Bauer, A., Papa, J.C., Whiteaker, K., Yates, D., Farsad, M., Marasco, P., Davies, M., and Rolland, J.P., "Increased Compactness of an Imaging Spectrometer Enabled by Freeform Surfaces," in Optical Design and Fabrication 2017 (Freeform, IODC, OFT), OSA Technical Digest (online), paper JW2C.5 (2017).
[5] Strese, H., and Maresi, L., "Technology developments and status of hyperspectral instruments at the European Space Agency", Proc. SPIE 11151, Sensors, Systems, and Next-Generation Satellites XXIII, 111510T
[6] Moreau, V., Borguet, B., Sharshavina, K., Bourdoux, A., Deep, A., and Santandrea, S., "Recent developments on free form optics based Spectro-imager for Small Sat Platform", The 4S Symposium (2018)
[7] Mouroulis, P., Wilson, D. W., Maker, P. D., and Muller, R. E., "Convex grating types for concentric imaging spectrometers", ppl. Opt. 37, 7200-7208 (1998)
[8] Mouroulis, P., "Low-distortion imaging spectrometer designs utilizing convex gratings," Proc. SPIE 3482, International Optical Design Conference 1998, (21 September 1998)
[9] Mouroulis, P, and Green, G. O., "Review of high fidelity imaging spectrometer design for remote sensing", Optical Engineering 57, 4, (2018)